Electronic Supplementary Material (ESI) for Journal of Materials Chemistry A.

Cooperative interaction between Cu and sulfur vacancies in SnS_2 nanoflower for highly efficient nitrate electroreduction to ammonia

Heen Li [a], Xiaoyue Xu [a], Xiaohu Lin[b], Shuheng Chen [a], Maoyue He [a], Fei Peng [b], Faming Gao* [a.c]

a. Key Laboratory of Applied Chemistry, Yanshan University, Qinhuangdao 066004, P. R. China

b. Analyses and Testing Center， Hebei Normal University of Science and Technology, Qinhuangdao 066000, P. R. China

c. Tianjin Key Laboratory of Brine Chemical Engineering and Resource Ecological Utilization, Tianjin University of Science & Technology, Tianjin 300222, P.R.China

Corresponding Author

*Faming Gao: E-mail: fmgao@ysu.edu.cn

Supporting information

Characterizations.

The microtopography of the prepared samples was characterized by transmission electron microscopy (TEM, JEOL 2100 plus + ARM 200 F). Energy dispersive X-ray spectroscopy attached to the transmission electron microscope was used to obtain elemental composition. Raman spectroscopy (WITec, alpha300R, excited by a 512 nm laser) was also performed. The crystalline phases were performed by X-ray diffraction (XRD) using an Rigaku D/MAX-2500 powder diffractometer. The chemical states of the prepared sample were conducted using a Thermo Scientific ESCALAB 250Xi photoelectron spectrometer. The absorbance data of spectrophotometer were collected on a SHIMADZU UV-2550 ultravioletvisible (UV-vis) spectrophotometer. Electron spin resonance (ESR) measurements were performed using the Bruker ER 200D spectrometer at room temperature.

Quantification of ammonia

When tested in alkaline solution, we used spectrophotometry method to detect the quantification of ammonia. Briefly, after 1h electrocatalysis, 0.2ml electrolyte was removed from cathode and diluted to 2 mL to detection range and following 2mL of 1M NaOH solution containing 5% salicylic acid and 5% sodium citrate was added into the solution. Subsequently, 1 mL of 0.05M NaClO and 0.2 mL of 1% $C_5FeN_6Na_2O{\cdot}2H_2O$ were add into the above solution. Then the solution was incubated under dark conditions at for 2h before UV-vis absorption spectrum was measured at a wavelength of 655 nm (Shimadzu, UV-2550). NH_4^+ calibration curve was calculated by using a series of different concentrations standard NH_3 Solution (0μg/mL,0.25μg/mL,0.5μg/mL,0.75μg/mL,1μg/mL).NH_4Cl was dried in oven before used. Calibration curve showed good linear relationship ($y=0.275x+0.02$ $R^2=0.9994$).

Quantification of nitrite

The color developer was configured as follows: 20 g of p-aminobenzenesulfonamide was added to a mixed solution of 250 ml of water and 50 ml of phosphoric acid, and then 1 g of N-(1-naphthyl)-ethylenediamine dihydrochloride was dissolved in the above solution. Finally, the above solution was transferred to a 500 mL volumetric flask and diluted to the mark. 1.0 mL electrolyte was taken out from the electrolytic cell and diluted to 5 mL to detection range. Next, 0.1 mL color reagent was added into the aforementioned 5 mL solution. After shaking and standing for 20 minutes, the absorbance was tested by UV-Vis spectrophotometry at a wavelength of 540 nm. The calibration curve can be obtained through different concentrations of $NaNO_2$ solutions and the corresponding absorbance. It showed an excellent linear relationship between the absorbance value and the $NaNO_2$ concentration from the fitting curve ($y = 0.768x + 0.034$ $R^2 = 0.9989$).

Calculation of the Faradaic efficiency and yield.

The Faradaic efficiency of NO_3RR was calculated as follows

$$FE = 3F \times c \times V / (17 \times Q)$$

where F is the Faraday constant, c is the measured NH_3 concentration, V is the volume of the electrolyte, and Q is the quantity of electric charge for one electron of NO_3RR testing.

The NH_3 formation rate was determined using the following equation:

$$r(NH_3) = (c \times V)/(t \times m)$$

where c is the measured NH_3 concentration, V is the volume of the electrolyte , t is the reduction reaction time, and m is the loading mass of sample (loading mass：0.25mg).

$K^{15}NO_3$ isotope labelling experiments

Isotopically labeled nitrate reduction experiments were conducted to elucidate the ammonia source and quantify the concentration of ammonia nitrogen using $K^{15}NO_3$ (99%) as the feed N source. After electrolyzing a 0.1 M KOH solution containing $K^{15}NO_3$ (0.1M KOH) for 2 h, electrolyte with $^{15}NH_4^+$ was extracted and the pH was further adjusted to weak acid by adding 4M H_2SO_4.Next, a 50 μL deuterium oxide (D_2O) was blended with 1mL of acidified electrolyte and the further ^1H NMR spectra was acquired via NMR analysis.

Calculation details

All calculations in this work were performed using the Vienna ab initio simulation package (VASP) based on the density functional theory (DFT). The projected augmented wave (PAW) method with PBE functional was employed for the generation of pseudopotential. The kinetic energy cutoff for the plane-wave expansion was set to 400 eV. The 3×3×1 k-point mesh set was used for pristine-SnS_2, SnS_{2-x} and Cu-SnS_{2-x} slab models. All the structural models were fully relaxed to the ground state with the convergence of energy and forces setting to 10-5 eV and 0.01 eV Å-1, respectively. SnS_2 (001) was modeled by a 4×4 supercell and a vacuum space of around 20 Å was set along the z-direction.

Here, the chemical reaction considered can be summarized with the reaction equations below.

$$*+ NO_3^- \rightarrow *NO_3 + e-$$

$$*NO_3 + 2H^+ + 2e^- \rightarrow *NO_2 + H_2O$$

$$*NO_2 + 2H^+ + 2e^- \rightarrow *NO + H_2O$$

$$*NO + 2H^+ + 2e^- \rightarrow *N + H_2O$$

$$*N + H^+ + e^- \rightarrow *NH$$

$$*NH + H^+ + e^- \rightarrow *NH_2$$

$$*NH_2 + H^+ + e^- \rightarrow *NH_3$$

$$*NH_3 \rightarrow NH_3 + *$$

where * represents the active site. Then, the reaction free energy change can be obtained with the equation below:

$$\Delta G = \Delta E + \Delta E_{ZPE} - T\Delta S$$

where ΔE is the total energy difference before and after intermediate adsorbed, ΔEZPE and ΔS are, respectively, the differences of zero point energy and entropy. The zero point energy and entropy of free molecules and adsorbents were obtained from the vibrational frequency calculations.

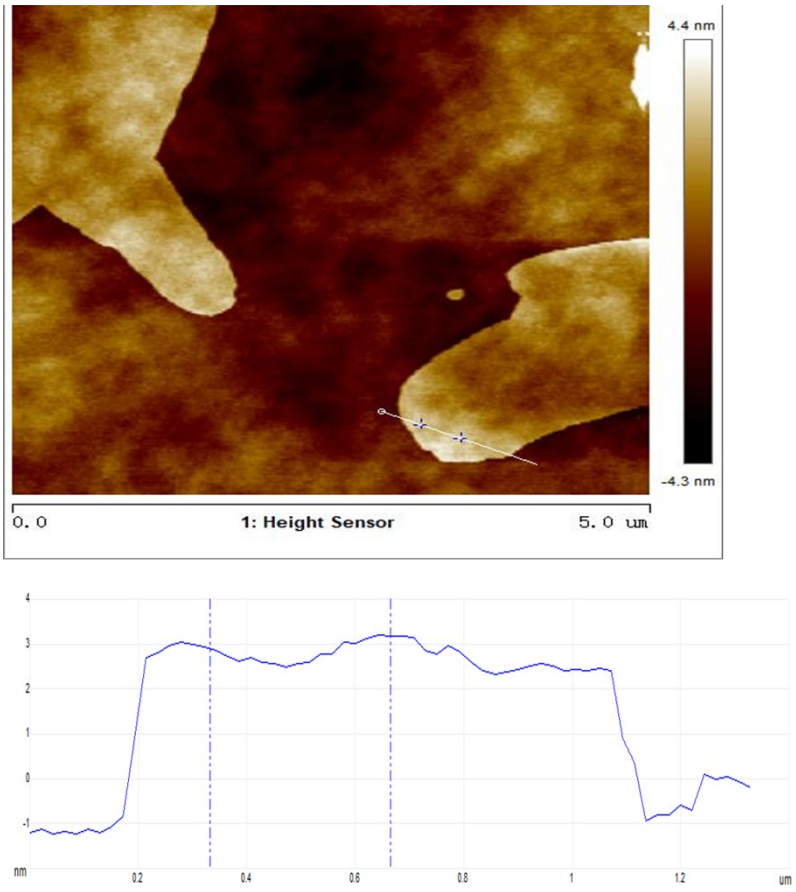

Fig. S1 AFM image of Cu-SnS_{2-x}

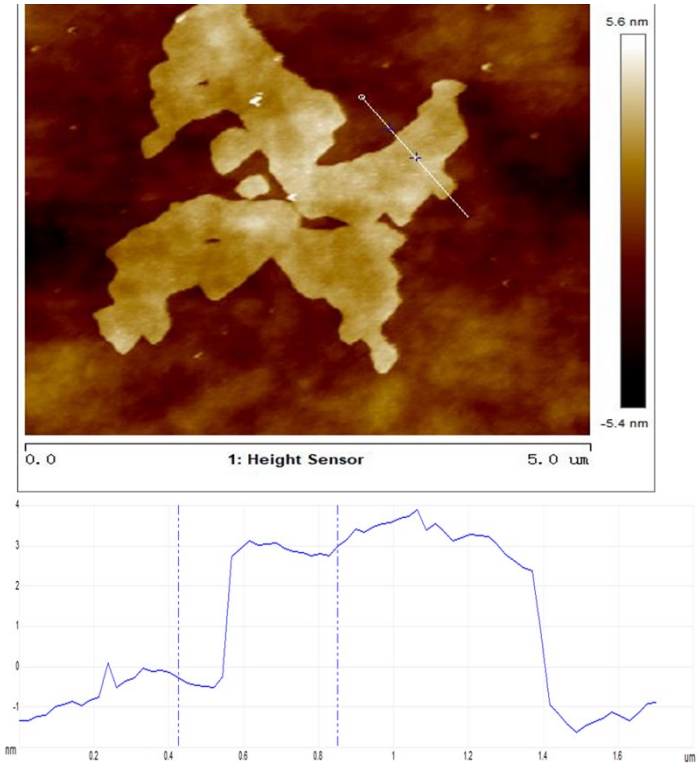

Fig. S2 AFM image of pristine-SnS_2

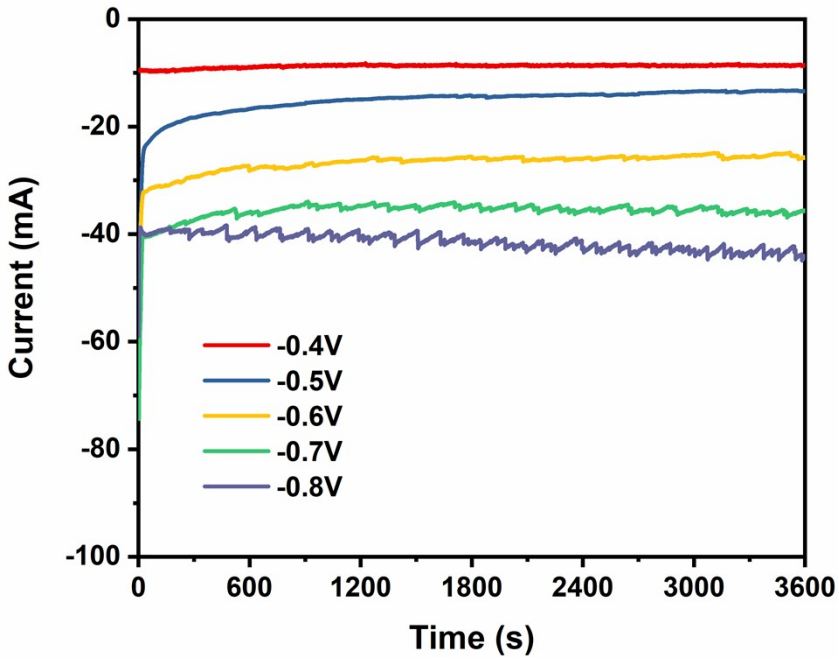

Fig. S3 Chronoamperometry curves of Cu-SnS_{2-x} at different potentials.

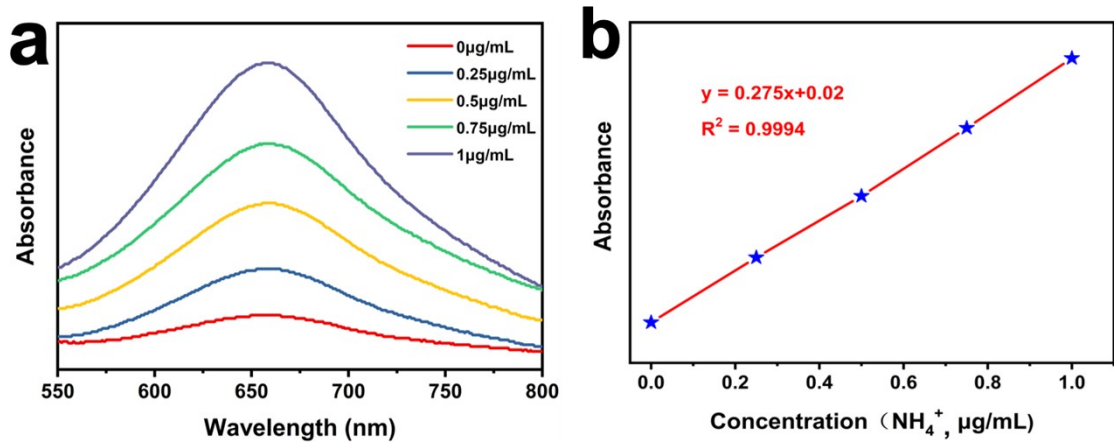

Fig. S4 (a) UV-Vis spectra of various NH_3 concentrations after incubated for 1 h at room temperature. (b) Calibration curve used for calculation of NH_3 concentrations.

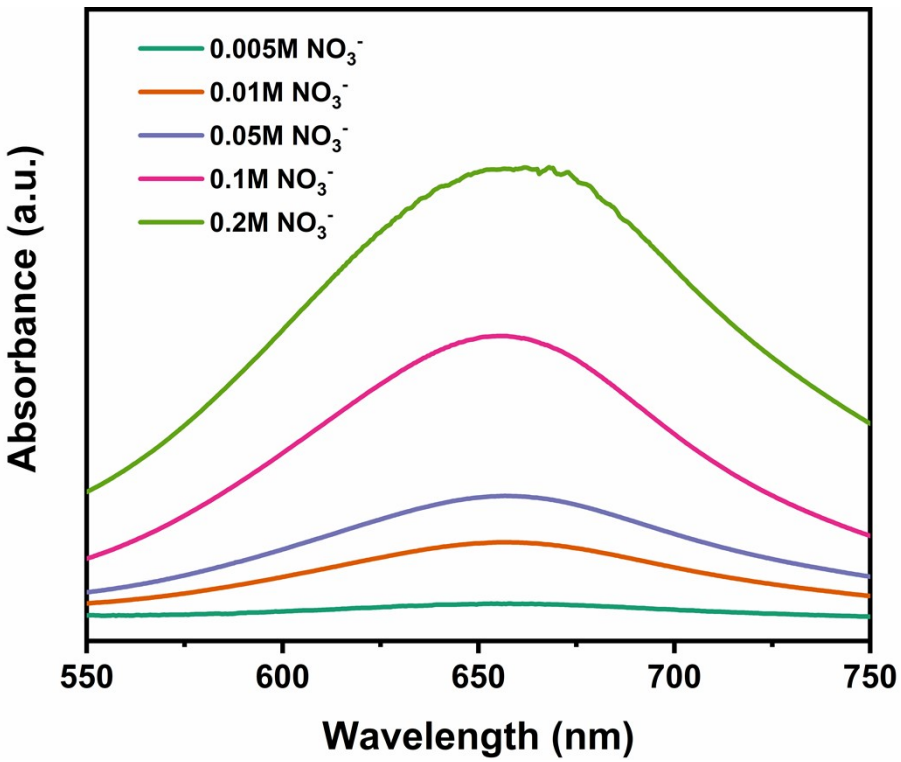

Fig. S5 UV-vis spectra of Cu-SnS_{2-x} at different NO_3^- concentrations.

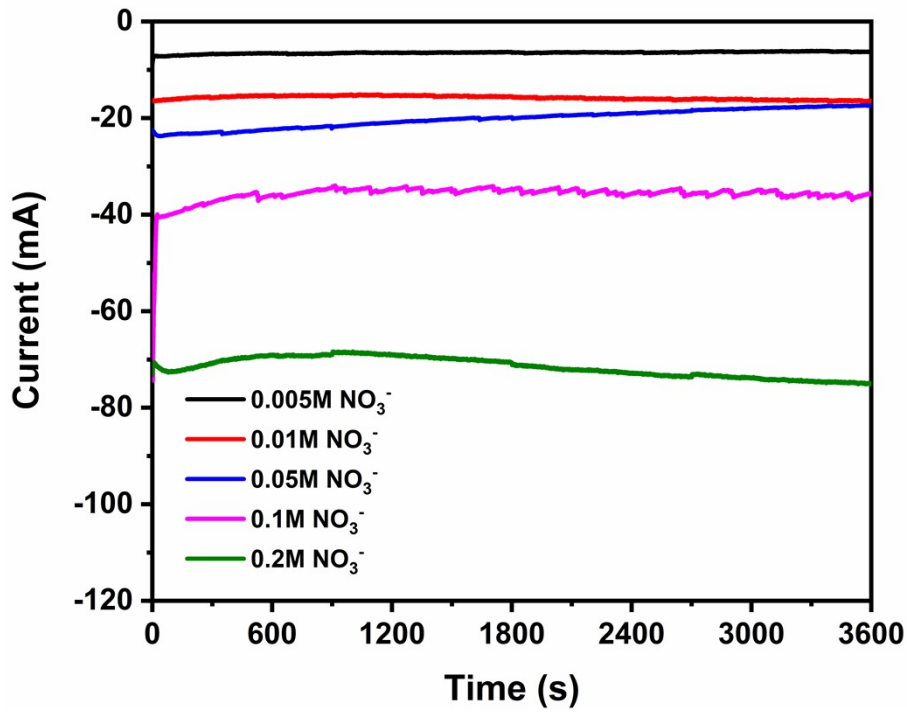

Fig. S6 Chronoamperometry curves of Cu-SnS_{2-x} at different NO_3^- concentrations.

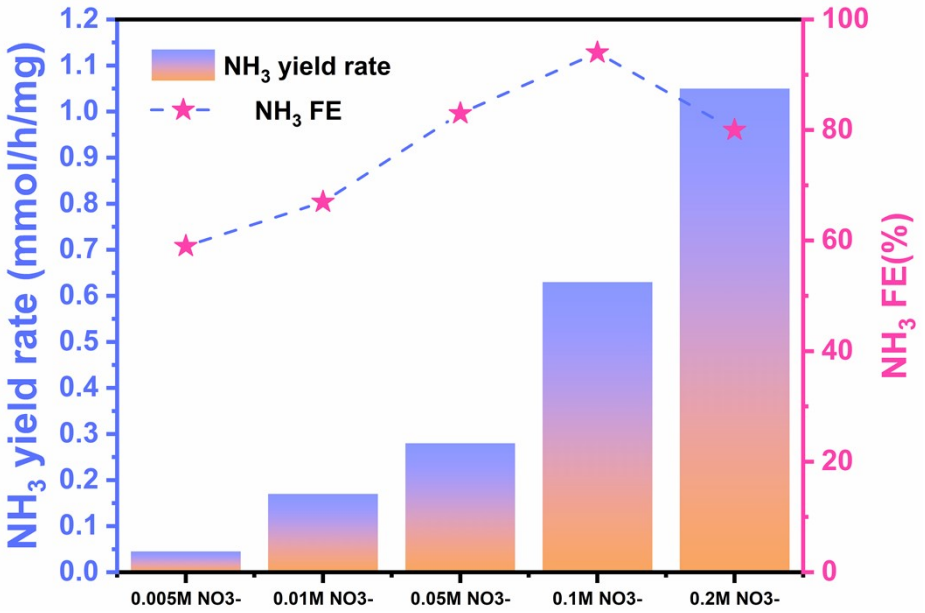

Fig. S7 NH_3 yields and FEs of Cu-SnS_{2-x} at different NO_3^- concentrations.

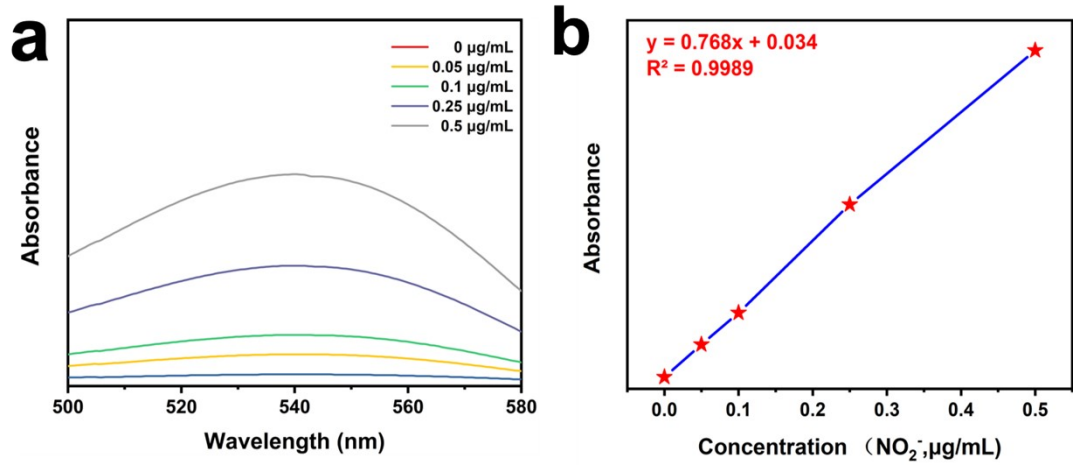

Fig. S8(a) UV-Vis spectra of various nitrite concentrations. (b) Calibration curve used for calculation of nitrite concentrations

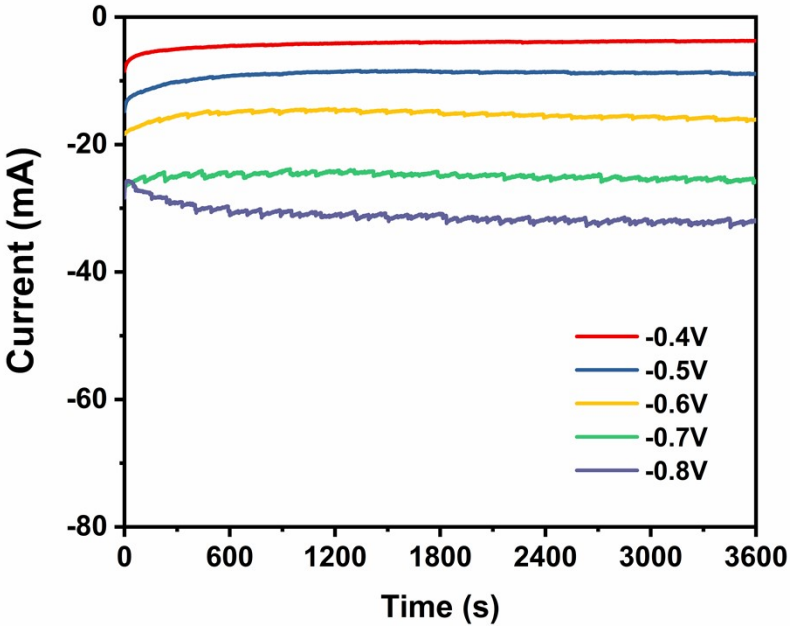

Fig. S9 Chronoamperometry curves of SnS_2 at different potentials.

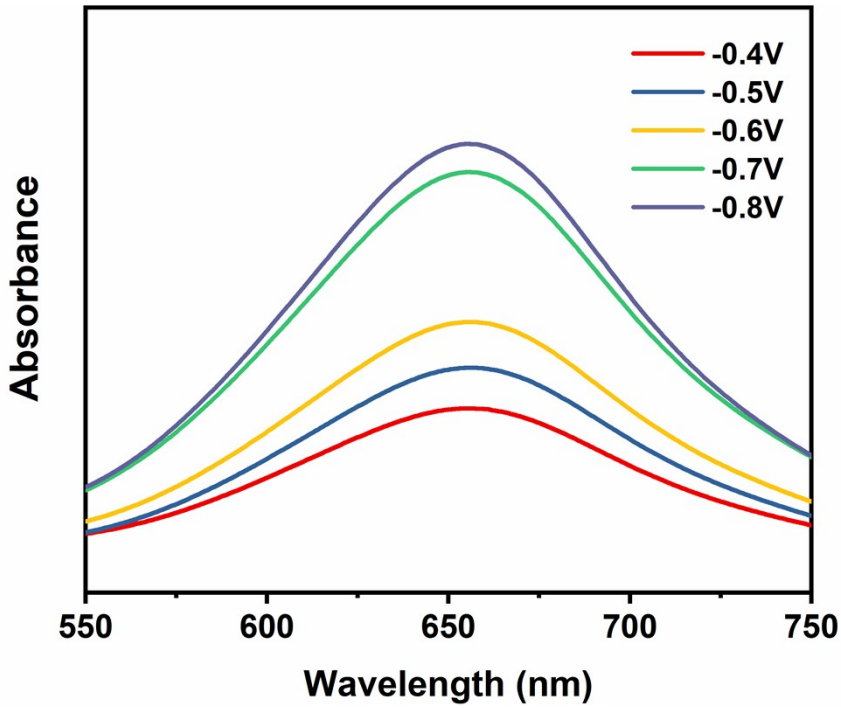

Fig. S10. UV-vis spectra of SnS_2 at different potentials

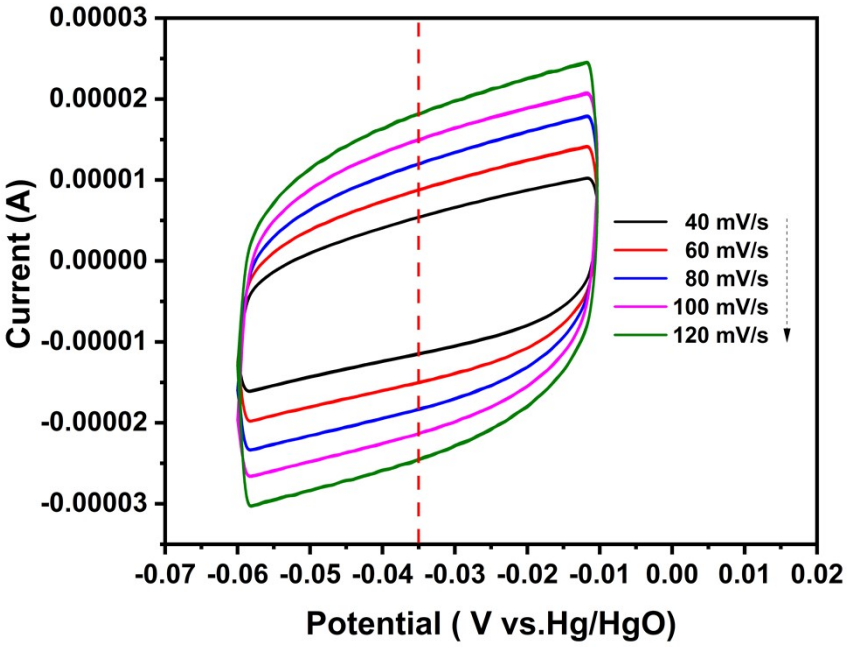

Fig. S11. CV curves of Cu-SnS_{2-x}

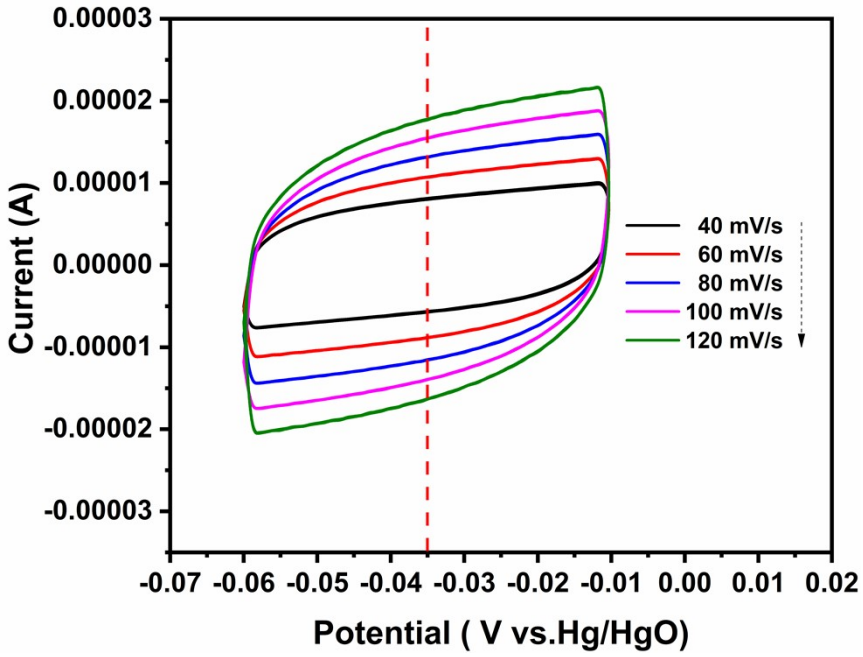

Fig. S12. CV curves of SnS_2

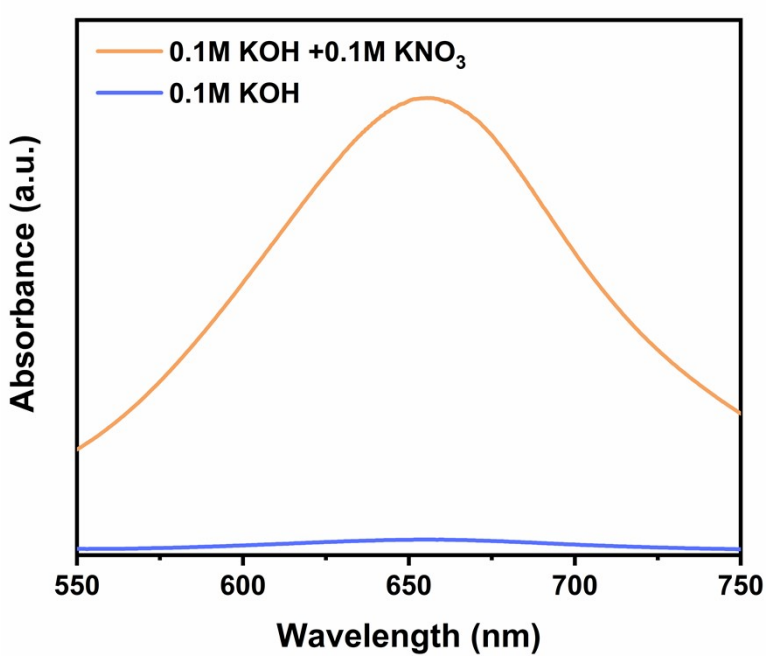

Fig. S13. UV-vis spectra of Cu-SnS_{2-x} tested in 0.1KOH and in 0.1MKOH + 0.1MKNO_3

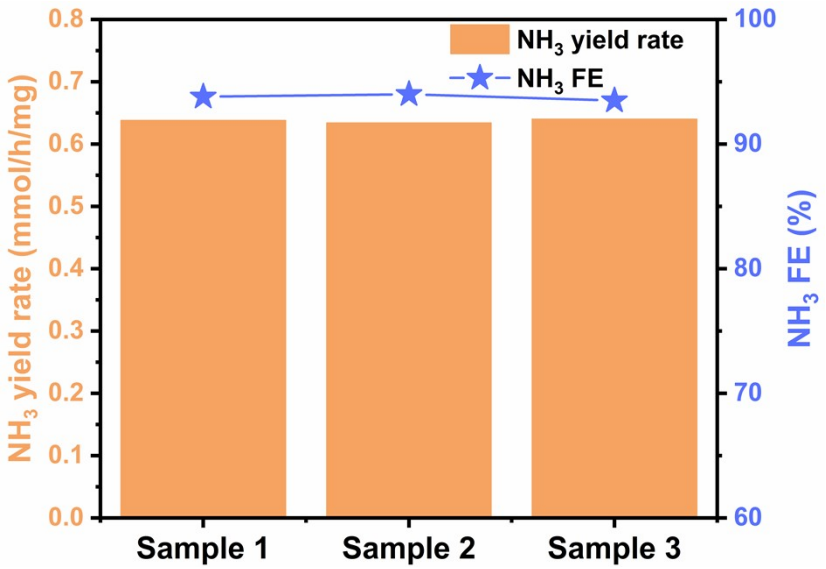

Fig. S14. NH_3 yields and FEs of three independent samples.

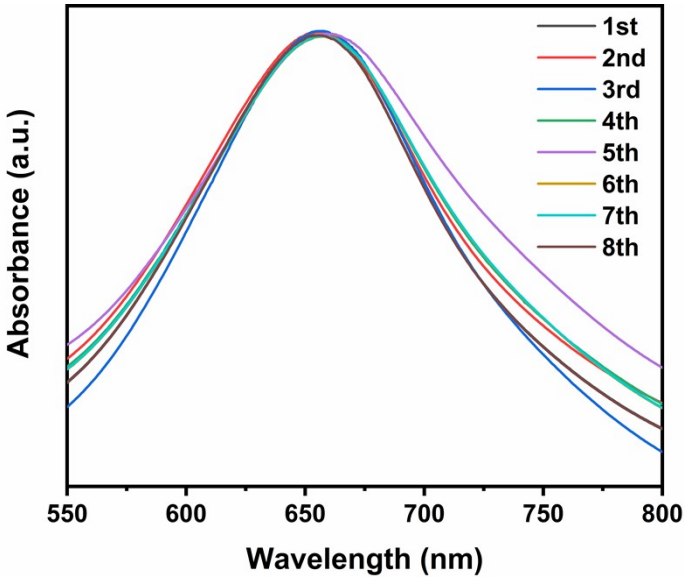

Fig. S15. UV-vis spectra of eight-times cycle test

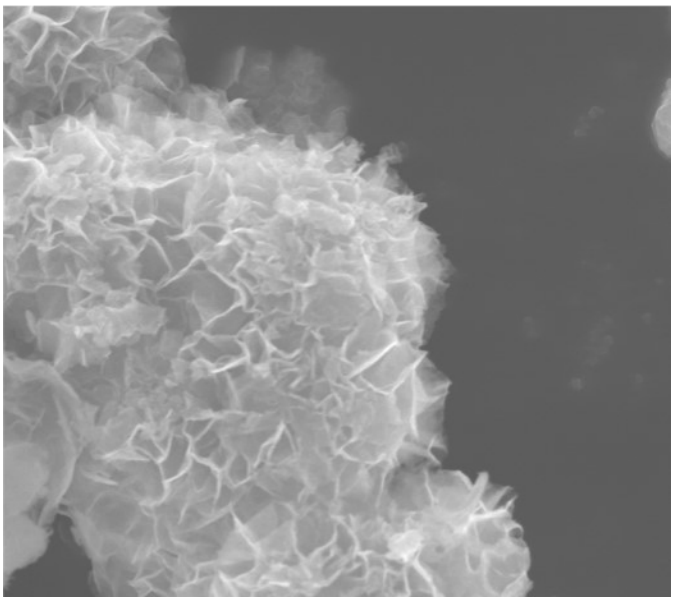

Fig. S16. SEM image of Cu-SnS_{2-x} after the cycle test

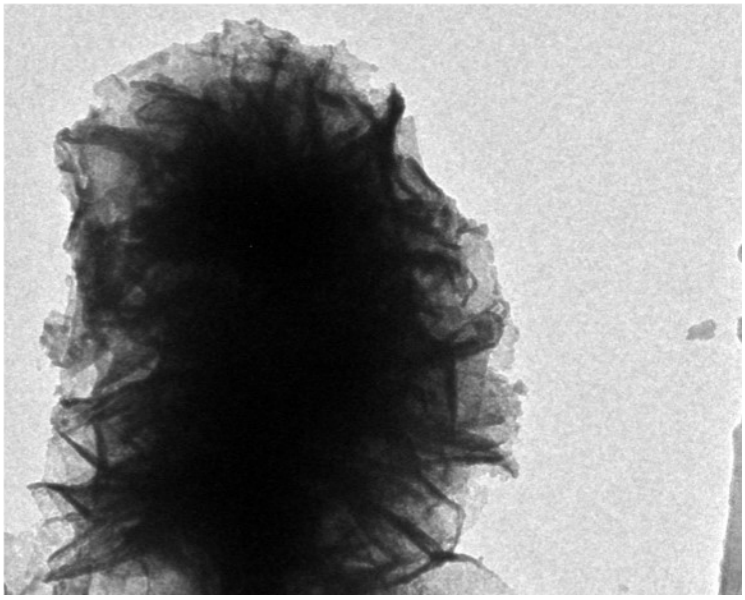

Fig. S17. TEM image of Cu-SnS_{2-x} after the cycle test

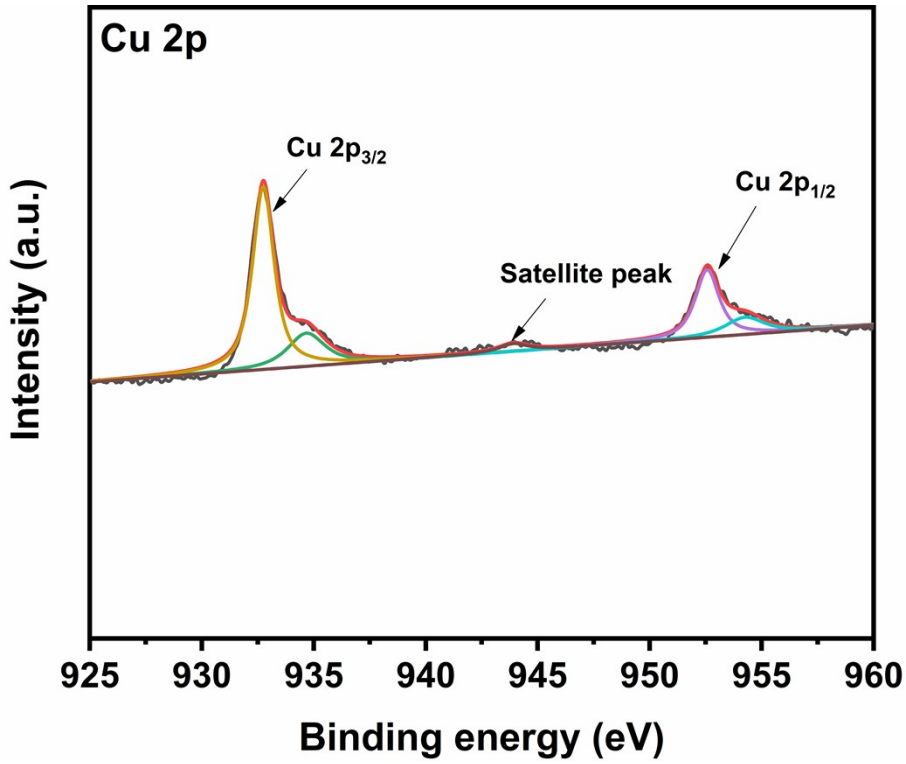

Fig. S18 XPS of Cu 2p after the cycle tests.

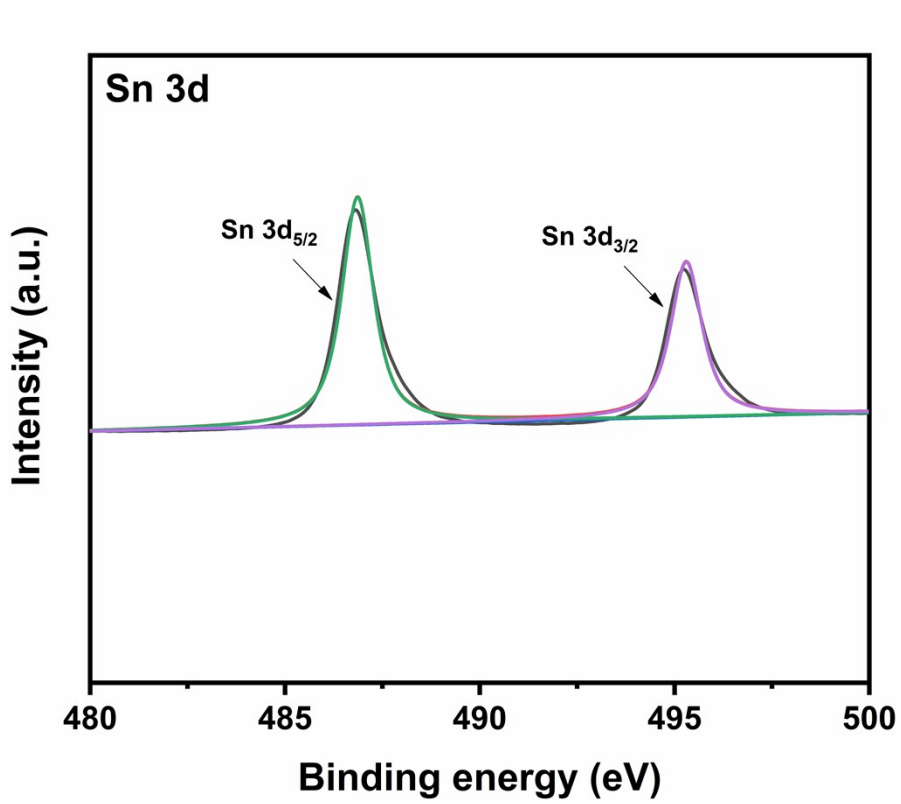

Fig. S19 XPS of Sn 3d after the cycle tests.

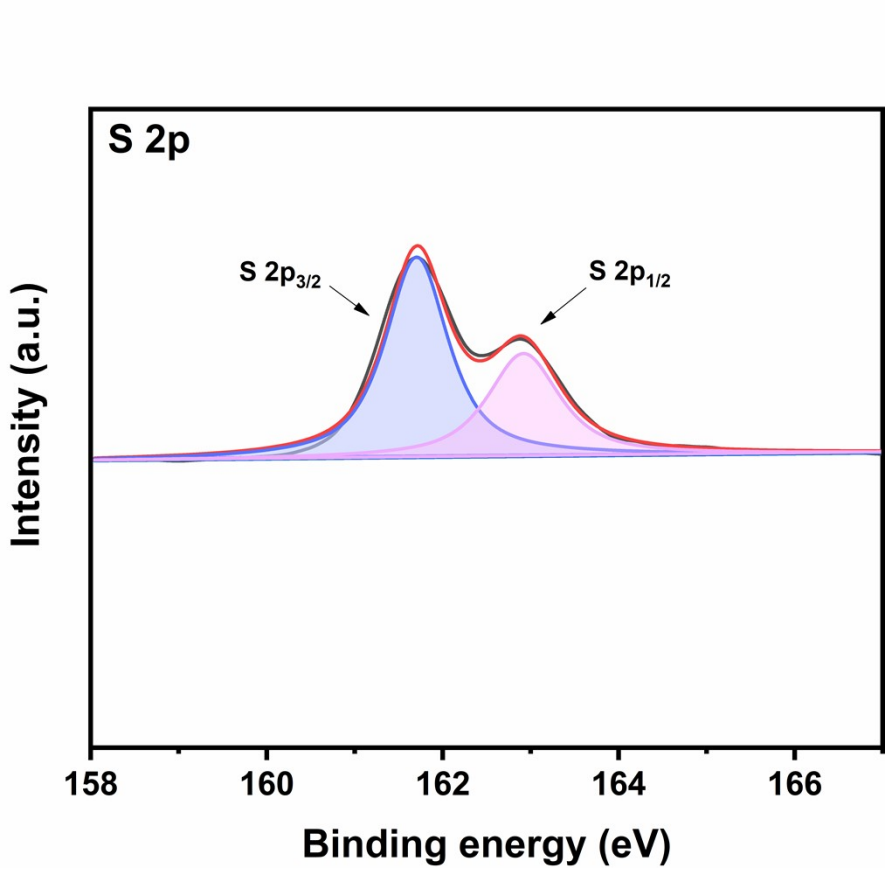

Fig. S20 XPS of S 2p after the cycle tests.

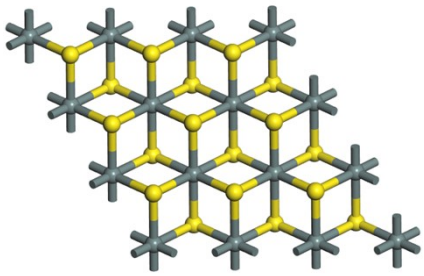

Fig.S21 Model of pristine-SnS_2 (Grey: Sn, yellow: S).

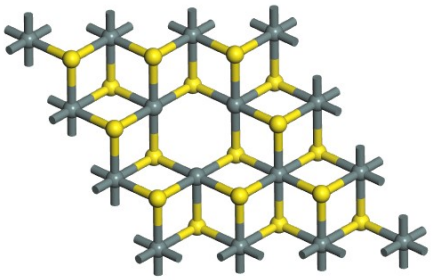

Fig.S22 Model of SnS_{2-x}(Grey: Sn , yellow: S).

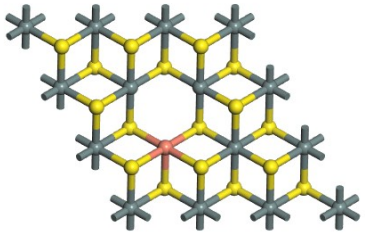

Fig.S23 Model of Cu-SnS_{2-x}(Grey: Sn, yellow: S, orange: Cu).

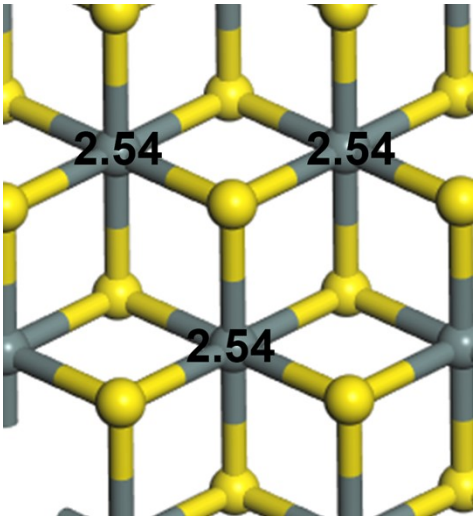

Fig.S24 Bader charge of pristine-SnS_2 (Grey: Sn , yellow: S).

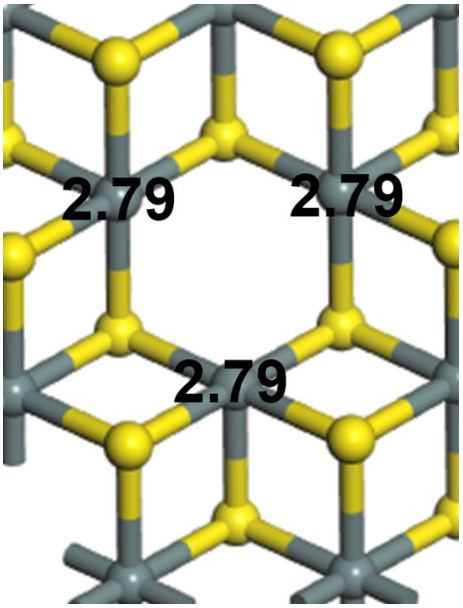

Fig.S25 Bader charge of SnS_{2-x} (Grey: Sn , yellow: S).

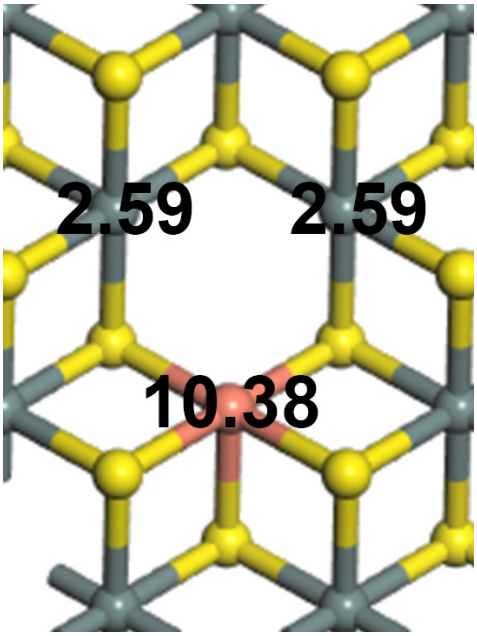

Fig.S26 Model of Cu-SnS_{2-x}(Grey: Sn, yellow: S, orange: Cu).

Table S1.Comparison with various electrocatalysts for NO_3RR.

Catalyst	NH_3 yield	FE(%)	Electrolyte	Ref.
Cu-SnS_{2-x}	0.63mmol/h/mg_{cat} (0.196mmol/h/cm^2)	93.8%	0.1MKOH+0.1M KNO_3	This work
Cu/Cu-Mn_3O_4 NSAs/CF	0.21mmol/h/ cm^2	92.4%	0.1MKOH+200ppm KNO_3	1
BCN@Cu	0.57mmol/h/mg_{cat}	89.3%	0.1MKOH+0.1M KNO_3	2
10Cu/TiO_{2-x}	0.1143mmol/h/mg_{cat}	81.34%	0.1MKOH+200ppm KNO_3	3
TiO_{2-x}	0.045mmol/h/mg_{cat}	85%	0.5MNa_2SO_4+50ppm KNO_3	4
Fe SAC	0.46mmol/h/ cm^2	75%	0.1MK_2SO_4+0.1M KNO_3	5
Cu/Pd/CuO_x	0.088mmol/h/mg_{cat}	84.04%	0.5MK_2SO_4+50ppm KNO_3	6
CuO@MnO_2/CF	0.24mmol/h/ cm^2	94.92%	0.5MK_2SO_4+200ppm KNO_3	7
$NiCo_2O_4$/CC	0.97mmol/h/ cm^2	99%	0.1MNaOH+0.1M $NaNO_3$	8

References

1. Wang, H.; Mao, Q.; Ren, T.; Zhou, T.; Deng, K.; Wang, Z.; Li, X.; Xu, Y.; Wang, L., Synergism of Interfaces and Defects: Cu/Oxygen Vacancy-Rich Cu-Mn_3O_4 Heterostructured Ultrathin Nanosheet Arrays for Selective Nitrate Electroreduction to Ammonia. *ACS Appl Mater Interfaces* 2021, *13* (37), 44733-44741.

2. Zhao, X.; Hu, G.; Tan, F.; Zhang, S.; Wang, X.; Hu, X.; Kuklin, A. V.; Baryshnikov, G. V.; Ågren, H.; Zhou, X.; Zhang, H., Copper confined in vesicle-like BCN cavities promotes electrochemical reduction of nitrate to ammonia in water. *Journal of Materials Chemistry A* 2021, *9* (41), 23675-23686.

3. Zhang, X.; Wang, C.; Guo, Y.; Zhang, B.; Wang, Y.; Yu, Y., Cu clusters/TiO_{2-x} with abundant oxygen vacancies for enhanced electrocatalytic nitrate reduction to ammonia. *Journal of Materials Chemistry A* 2022, *10* (12), 6448-6453.

4. Jia, R.; Wang, Y.; Wang, C.; Ling, Y.; Yu, Y.; Zhang, B., Boosting Selective Nitrate Electroreduction to Ammonium by Constructing Oxygen Vacancies in TiO_2. *ACS Catalysis* 2020, *10* (6), 3533-3540.

5. Wu, Z. Y.; Karamad, M.; Yong, X.; Huang, Q.; Cullen, D. A.; Zhu, P.; Xia, C.; Xiao, Q.; Shakouri, M.; Chen, F. Y.; Kim, J. Y. T.; Xia, Y.; Heck, K.; Hu, Y.; Wong, M. S.; Li, Q.; Gates, I.; Siahrostami, S.; Wang, H., Electrochemical ammonia synthesis via nitrate reduction on Fe single atom catalyst. *Nat Commun* 2021, *12* (1), 2870.

6. Ren, T.; Yu, Z.; Yu, H.; Deng, K.; Wang, Z.; Li, X.; Wang, H.; Wang, L.; Xu, Y., Interfacial polarization in metal-organic framework reconstructed Cu/Pd/CuOx multi-phase heterostructures for electrocatalytic nitrate reduction to ammonia. *Applied Catalysis B:*

Environmental 2022, *318*.

7. Xu, Y.; Sheng, Y.; Wang, M.; Ren, T.; Shi, K.; Wang, Z.; Li, X.; Wang, L.; Wang, H., Interface coupling induced built-in electric fields boost electrochemical nitrate reduction to ammonia over CuO@MnO_2 core–shell hierarchical nanoarrays. *Journal of Materials Chemistry A* 2022, *10* (32), 16883-16890.

8. Liu, Q.; Xie, L.; Liang, J.; Ren, Y.; Wang, Y.; Zhang, L.; Yue, L.; Li, T.; Luo, Y.; Li, N.; Tang, B.; Liu, Y.; Gao, S.; Alshehri, A. A.; Shakir, I.; Agboola, P. O.; Kong, Q.; Wang, Q.; Ma, D.; Sun, X., Ambient Ammonia Synthesis via Electrochemical Reduction of Nitrate Enabled by $NiCo_2O_4$ Nanowire Array. *Small* 2022, *18* (13), e2106961.